Enhanced hydrogen desorption properties of magnesium hydride by coupling non-metal doping and nano-confinement

Daliang He, Yulong Wang, Chengzhang Wu' , Qian Li, Weizhong Ding, and Chenghua Sun'

Citation: Appl. Phys. Lett. **107**, 243907 (2015); doi: 10.1063/1.4938245
View online: http://dx.doi.org/10.1063/1.4938245
View Table of Contents: http://aip.scitation.org/toc/apl/107/24
Published by the American Institute of Physics

Enhanced hydrogen desorption properties of magnesium hydride by coupling non-metal doping and nano-confinement

Daliang He,[1] Yulong Wang,[1] Chengzhang Wu,[1,a)] Qian Li,[1,2] Weizhong Ding,[1] and Chenghua Sun[3,a)]
[1]State Key Laboratory of Advanced Special Steel, Shanghai University, Shanghai 200072, China
[2]Institute of Genomic Material, Shanghai University, Shanghai 200444, China
[3]School of Chemistry, Monash University, Clayton, Victoria 3800, Australia

(Received 9 November 2015; accepted 8 December 2015; published online 18 December 2015)

Magnesium hydride (MgH_2) offers excellent capacity to store hydrogen, but it suffers from the high desorption temperature (>283 °C for starting release hydrogen). In this work, we calculated the hydrogen desorption energy of $Mg_{76}H_{152}$ clusters with/without non-metal dopants by density functional theory method. Phosphorus (P), as identified as the best dopant, can reduce the reaction energy for releasing one hydrogen molecule from 0.75 eV (bulk MgH_2) to 0.20 eV. Inspired by the calculation, P-doped ordered mesoporous carbon (CMK-3) was synthesized by one-step method and employed as the scaffold for loading MgH_2 nanoparticles, forming MgH_2@P/CMK-3. Element analysis shows that phosphorus dopants have been incorporated into the CMK-3 scaffold and magnesium and phosphorus elements are well-distributed in carbon scaffold hosts. Tests of hydrogen desorption confirmed that P-doping can remarkably enhance the hydrogen release properties of nanoconfined MgH_2 at low temperature, specifically ~1.5 wt. % H_2 released from MgH_2@P/CMK-3 below 200 °C. This work, based on the combination of computational calculations and experimental studies, demonstrated that the combined approach of non-metal doping and nano-confinement is promising for enhancing the hydrogen desorption properties of MgH_2, which provides a strategy to address the challenge of hydrogen desorption from MgH_2 at mild operational conditions. © *2015 AIP Publishing LLC*. [http://dx.doi.org/10.1063/1.4938245]

Hydrogen (H_2) has been regarded as an ideal energy carrier with nearly zero pollution and high energy density (142 MJ/kg).[1,2] One of the key challenges towards the large scale use of H_2 fuel is the storage. Among numerous storage materials, magnesium hydride (MgH_2) has attracted extensive attention due to its high capacity (7.6 wt. % H_2) and low cost.[3,4] Nevertheless, the practical application of Mg is still restricted by the sluggish kinetics and high desorption temperature (T_{des}). To address this issue, various technologies have been developed, such as doping, ball milling, and nano confinement.[5–17] For instance, T_{des} can be reduced remarkably if ultra-small MgH_2 nanoparticles are employed, like 0.9 nm corresponding to $T_{des} \approx 200$ °C,[7–9] but the disadvantage is that such small particles would be sintered or aggregated during the following hydrogen absorption and desorption cycles. To get over this problem, nano-confinement strategy has been proposed—MgH_2 nano particles are confined in porous scaffolds, such as metal organic framework (MOF),[10] ordered mesoporous carbon (CMK-3),[11–13] carbon aerogel,[14] and mesoporous silicon.[15,16] Very recently, Jia *et al.*[17] loaded MgH_2 into CMK-3, in which case hydrogen release can start even from only 50 °C. Besides the effect of nano-confinement, the authors proposed that the charge transfer from MgH_2 to the carbon scaffold plays a critical role in the significant improvement of MgH_2 dehydrogenation. Inspired by this work, we speculated that better performance may be achievable when the interfacial bonding between magnesium and the confinement environment is further optimized. In terms of the modification of carbon scaffold, doping with non-metal heteroatoms as a technique has been widely employed in the literatures.[18,19] The basic idea is that heteroatoms incorporated into carbon network can result in local distortion and change the original electron distribution, and consequently activate a part of carbon atoms. This letter reports our computational investigation and experimental validation of phosphorus (P)-modified CMK-3 as the scaffold for MgH_2 (named as MgH_2@P/CMK-3).

We start from a computational investigation of four non-metal dopants (X = B, N, S, and P), with a focus on whether these heteroatoms can destabilize MgH_2 confined by CMK-3 scaffold. The calculations were performed under the scheme of standard density functional theory (DFT) with Perdew–Burke–Ernzerhof functional for the exchange-correlation term,[20] as embedded in the Vienna *ab-initio* Simulation Package (VASP).[21] During the calculation, the projector augmented wave method[22] with a cutoff energy of 400 eV has been employed to achieve high computational efficiency. CMK-3 is modeled by a cubic supercell with a pore, being same as the work by Jia *et al.*,[17] as shown in Fig. 1(a), in which dopants (blue spheres) are introduced to replace carbon atoms, followed by full relaxation with MgH_2 or Mg clusters. The desorption energy (DE) is calculated by $DE = (E(MgH_2@C) - E(Mg@C) - nE(H_2))/n$, where $E(MgH_2@C)$ and $E(Mg@C)$ are the energy of MgH_2 and Mg clusters confined in CMK-3, and $E(H_2)$ and n are the energy of single H_2 molecule and the number of H_2 released from the system. Given the desorption of surface hydrogen and bulk hydrogen is quite different, our calculations only

a)Electronic mail: wucz@shu.edu.cn and chenghua.sun@monash.edu

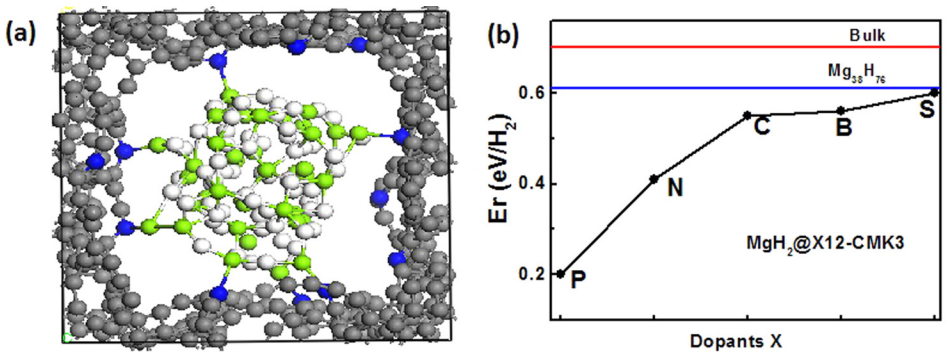

FIG. 1. Computational screening of dopants. (a) Model of CMK-3 filled with MgH_2 cluster, with C, Mg, and H being shown as gray, green, and white spheres and dopants (X) shown as blue spheres. (b) Calculated average value of desorption energy Er with X = P, N, B, and S, with the data for bulk case, pure $Mg_{38}H_{76}$ cluster, and undoped (X = C) structures listed as reference.

consider the averaged DE with hydrogen being fully released.

Fig. 1(b) shows the calculated DE, with the data of bulk MgH_2 and unconfined cluster $Mg_{76}H_{152}$ as the reference. For bulk MgH_2, DE is as high as 0.75 eV per H_2, as determined by the strong Mg-H bonding. For $Mg_{76}H_{152}$ clusters, DE is reduced to 0.62 eV with respect to the bulk case, whose improvement is made due to the size effect. When it is confined in CMK-3 (corresponding to X = C), DE can be further reduced to 0.55 eV, due to the confinement effect. Among the four dopants, only N and P can reduce DE further, especially P-dopants can achieve an impressive DE = 0.2 eV per H_2.

To validate the computational predication, we turn to the synthesis of P-modified CMK-3 as a scaffold to confine MgH_2 clusters. Experimentally, a one-step nano-casting method has been employed to synthesize high surface area P/CMK-3 using SBA-15 as a hard template.[17,18] Briefly, the carbon replica was prepared by infiltrating the mesopores of 1.0 g of SBA-15 with 1.25 g of sucrose dissolved in 5.0 ml of water containing 0.14 g of H_2SO_4 and 0.5 g of H_3PO_4 at the room temperature. The obtained composite was dried at 100 °C for 12 h and at 160 °C for another 12 h, and subsequently was completely carbonized at 850 °C for 5 h in a nitrogen atmosphere. After carbonization, the SBA-15 template was removed by etching the replica in a 7.5% HF solution to obtain silica-free P/CMK-3 scaffold. Then, MgH_2@P/CMK-3 was synthesized following a study reported by Zhang *et al.*[23] The P/CMK-3 scaffold with 20 ml of $MgBu_2$ solution was first sealed into an autoclave and hydrogenated at 170 °C under a H_2 pressure of 50–55 bar, and the MgH_2 incorporated P/CMK-3 was obtained after drying MgH_2 precipitate. Additionally, MgH_2 incorporated CMK-3 (non-P doping) was also prepared for comparison, named as MgH_2@CMK-3. Microstructural characteristics were evaluated using X-ray diffractometer (XRD, Rigaku D/MAX-2200) and transmission electron microscopy (JEOL JEM-2010 F). N_2 sorption isotherms were measured using nitrogen adsorption apparatus (ASAP 2020). X-ray photoelectron spectroscopy (XPS, ESCALAB 250Xi, UK) was used in the surface analysis. Hydrogen desorption properties were examined using a temperature programmed desorption with mass spectrometry (TPD-MS, Hiden HPR20) measurement and a home-made Sieverts' PCT apparatus.[5]

The surface area and pore size of the synthesized MgH_2@CMK-3 and MgH_2@P/CMK-3 samples were determined by N_2 adsorption–desorption isotherms. The N_2 sorption analysis of CMK-3 and P/CMK-3 shows a representative type IV isotherm, indicating a high uniformity of mesopores. After P-doping, the Brunauer–Emmett–Teller (BET) surface area declines slightly, from 1423 m^2/g of CMK-3 to 1044 m^2/g of P/CMK-3. In addition, when MgH_2 nanoparticles were loaded into the carbon scaffold, BET surface area decreased remarkably, down to 600 m^2/g and 359 m^2/g for MgH_2/CMK-3 and MgH_2@P/CMK-3, respectively. Moreover, after MgH_2 loading into the P doped/non-doped carbon scaffolds, only one third of pore volume remains in both cases. Decreased BET surface area and pore volume suggest that the mesoporous structure was degraded as a result of MgH_2 highly confined in the carbon mesopores, which is in good agreement with the previous study.[17]

The doping of phosphorus onto the ordered mesoporous carbon framework was verified by the XPS measurements. The XPS survey spectrum of P-doped CMK-3 given in Fig. 2(a) shows a predominant peak at 284.4 eV corresponding to C1s, a peak at 532.4 eV to O1s, and a peak at 133.5 eV to P2p.[18,19] Quantitative XPS analysis shows that phosphorus is present with ~5.48%, which is much higher than the value obtained from chemical analysis result (1.82 at. %). As a tool of surface analysis, XPS gives the element composition just on the surface with several nanometers depth, but chemical analysis shows an average content in the whole sample. As shown in Fig. 2(b), the high-resolution C1s XPS spectrum can be split into two different components located at about 284.4 and 285.6 eV, which can be attributed to C–C and C–P bonding, respectively.[18,19] The presence of the C–P peak confirms that P atoms have been intercalated into the carbon lattice. The O1s peak shown in Fig. 2(c) can be split into three component peaks, at 530.7 eV, 531.7 eV, and 532.8 eV, corresponding to physically absorbed oxygen molecules,[24,25] P–O bonding, and C-O bonding,[25] respectively. The high-resolution P2p spectrum (Fig. 2(d)) reveals that phosphorus was doped into carbon network in two main types of chemical bondings: P–C and P–O bondings at about 133.2 eV and 134.4 eV, respectively.[18,19,25] The above results confirm that the phosphorus atoms are incorporated into the CMK-3 framework.

HR-TEM measurement was also carried out on the synthesized P/CMK-3 and MgH_2@P/CMK-3. As shown in Fig. 3(a), a pore size of around 4.0 nm in diameter can be observed in the ordered mesoporous P/CMK-3, and such ordered mesopores of P/CMK-3 are filled by MgH_2 nanoparticles after hydride loading (Fig. 3(b)). The finding is consistent with the observation shown in the N_2 sorption isotherms, e.g., both BET surface area and pore volume are remarkably decreased when MgH_2 is loaded. To further

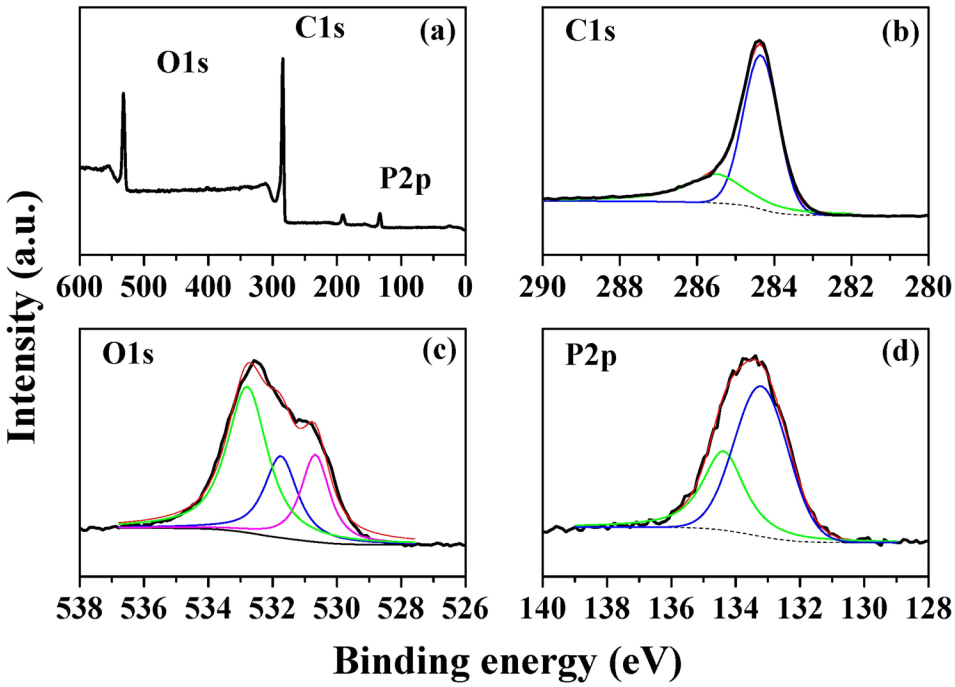

FIG. 2. XPS survey (a) and high resolution C1s (b), O1s (c), and P2p (d) spectra of as-prepared P-doped CMK-3 sample.

confirm the dispersion of confined MgH_2 nanoparticles, element mapping of Mg and P was analyzed by Energy Dispersive X-Ray Spectroscopy (EDX), and the results are given in Figs. 3(c) and 3(d), indicating that MgH_2 nanoparticles are well-distributed in P/CMK-3 scaffold hosts.

To further verify the effect of P-doping on the hydrogen desorption property of the nanoconfined MgH_2, the hydrogen desorption behavior of MgH_2@CMK-3 and MgH_2@P/CMK-3 were examined using TPD-MS and volumetric method. The TPD-MS profiles and hydrogen desorption kinetics curves are shown in Figs. 4(a) and 4(b), respectively. Here, the as-prepared CMK-3 was also hydrogenated under H_2 with a pressure of 55 bar at 170 °C, at the same condition as the hydrogenation procedure of $MgBu_2$. As shown in Fig. 4(a), the sample of MgH_2@CMK-3 starts to release hydrogen at ~50 °C, being consistent with the reference,[17] but the hydrogen release rate is very slow at the temperature lower than 280 °C. At the temperature above 280 °C, the hydrogen desorption rate speeds up obviously, and desorption peak is centered at ~380 °C. In comparison of MgH_2@CMK-3, the hydrogen release rate of the sample of MgH_2@P/CMK-3 is much faster at the low temperature zone (30 °C–280 °C), which indicates that the P-doping could enhance the hydrogen desorption from MgH_2, particularly at relatively low temperature. In addition, as a reference, the hydrogen signal of hydrogenated CMK-3 was also

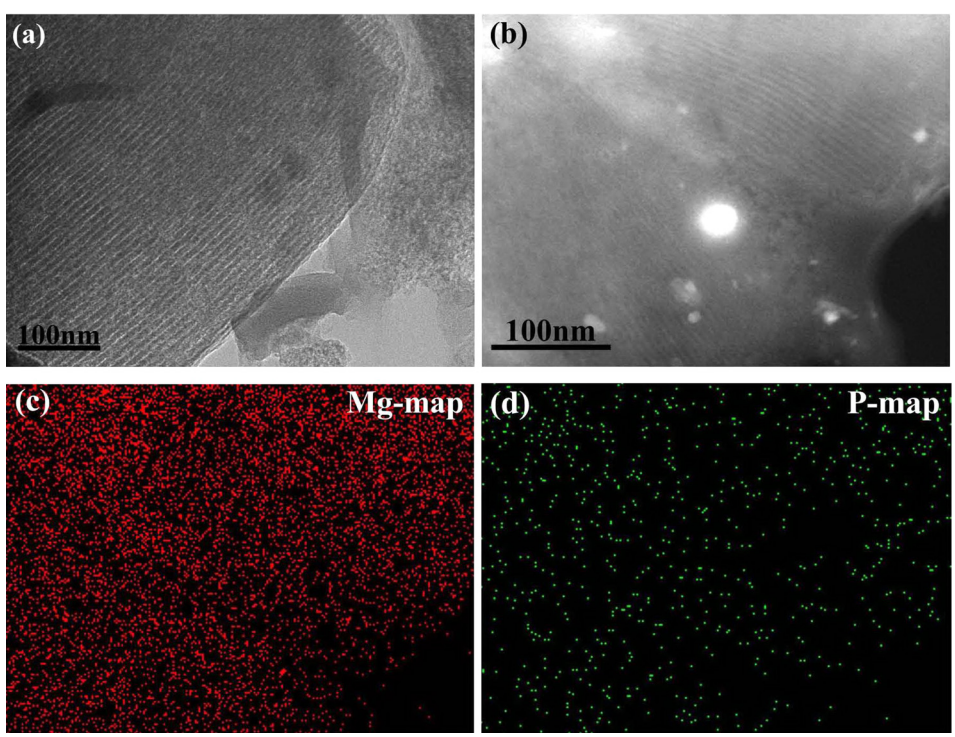

FIG. 3. HRTEM image of (a) P/CMK-3 and (b) MgH_2@P/CMK-3. The element mapping of (c) Mg and (d) P through the sample of MgH_2@P/CMK-3.

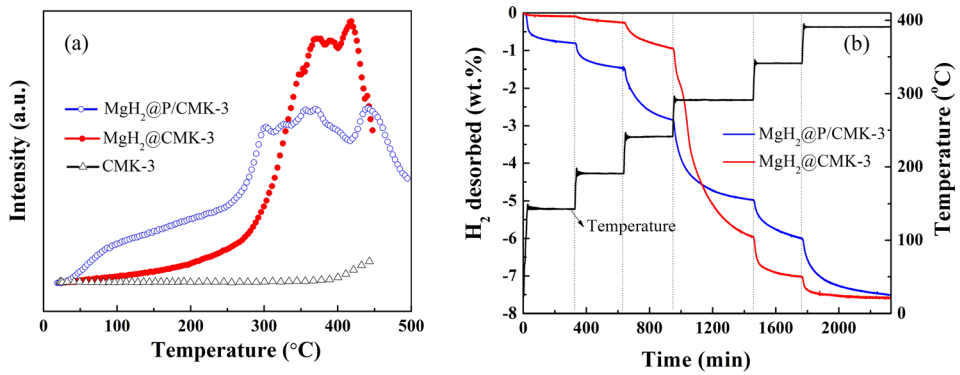

FIG. 4. (a) TPD-MS spectra of MgH_2@CMK-3, MgH_2@P/CMK-3, and CMK-3 measured with a heating rate of 5 °C/min under Ar flowing gas. (b) Hydrogen desorption kinetics curves of MgH_2@CMK-3 and MgH_2@P/CMK-3 measured at the temperature from room temperature to 143 °C, 191 °C, 241 °C, 291 °C, 341 °C, and 391 °C and kept different times (heating rate 10 °C/min). For comparison, the theoretical hydrogen content of pure MgH_2 (7.6 wt. %) was designated as the maximum of hydrogen release capacity.

examined by TPD-MS, in which case almost no hydrogen has been released before the temperature increases to 400 °C (Hydrogen signal above 400 °C indicates that $-CH_2$ or $-CH_3$ functional group may be formed during hydrogenation of CMK-3, which is different from the as-prepared CMK-3 reported by Jia *et al.*[17]). The above result proved that the hydrogen released at the low temperature comes from the decomposition of MgH_2, and P-doping can enhance the low-temperature hydrogen release.

In order to gain further insight into the hydrogen desorption behavior of MgH_2 by coupling P-doping and nanoconfinement, volumetric method was applied for the hydrogen desorption kinetics measurement. Fig. 4(b) presents hydrogen desorption kinetics curves of the samples of MgH_2@CMK-3 and MgH_2@P/CMK-3 at various temperatures. Here, for the comparison of the hydrogen desorption behavior of hydrogenated phase (MgH_2) in the two samples, the theoretical hydrogen content of pure MgH_2 (7.6 wt. %) was designated as the maximum of hydrogen release capacity. Notably, the sample of MgH_2@P/CMK-3 released about 0.8 wt. % H_2 below 150 °C, 1.5 wt. % H_2 below 200 °C, and 2.8 wt. % H_2 below 250 °C. Correspondently, the sample of MgH_2@CMK-3 released only about 0.1, 0.3, and 0.9 wt. % H_2 at the same conditions. It is noteworthy that the sample of MgH_2@P/CMK-3 exhibits much better desorption behavior than MgH_2@CMK-3 at low temperature region (below 250 °C). Whereas, when the temperature is higher than 250 °C, MgH_2@CMK-3 shows faster hydrogen desorption rate than the sample of MgH_2@P/CMK-3, which is in good agreement with TPD-MS result. The opposite behavior in hydrogen release at the high temperature zone should be caused by the distinguishing porous structure. We know that the BET surface area of MgH_2@P/CMK-3 (359 m^2/g) is almost half in comparison with that of MgH_2@CMK-3 (600 m^2/g). Thus, we speculate that the hydrogen desorption of the nanoconfined MgH_2 might be mainly affected by two factors: one is the heteroatom doping on the carbon scaffold; the other one is the surface area of the carbon scaffold. On the one hand, P-doping would enhance the hydrogen desorption properties of nanoconfined MgH_2. However, in this study, P-doped content is only 1.82 wt. %, which means that the destabilization of Mg-H bond by P atoms may not be sufficient. On the other hand, the higher the BET surface of porous carbon, the more the MgH_2 particles embedded in the scaffold, which implies that MgH_2@CMK-3 sample with higher BET surface should have better desorption performance due to nano-confinement effect. However, in this study, the decrement of DE by P-doping can improve the thermodynamics of hydrogen desorption, which means that phosphorus doping may have stronger influence at low temperature zone comparing with BET surface. In addition, the hydrogen absorption/desorption cycle property of the MgH_2@P/CMK-3 was also studied. We found that the hydrogen capacity of the sample could be recycled without any deterioration. Nevertheless, the above results also generate other questions for us, such as the influences of phosphorus doping content, oxygen content in CMK-3, porous structure of carbon scaffold, etc., and the detailed experiments are now in progress.

In conclusion, the hydrogen desorption energy of MgH_2@X/CMK-3 was computationally studied by DFT method. The phosphorus, as identified as the best dopant, can reduce the reaction energy from 0.75 eV (bulk MgH_2) to 0.20 eV for the release of one H_2. Experimentally, P-doped CMK-3 has been synthesized by one-step method and employed to host MgH_2 nanoparticles. Both TPD-MS and hydrogen kinetics desorption results proved that P-doping can remarkably enhance the hydrogen release properties of nanoconfined MgH_2 at low temperature. Particularly, about 1.5 wt. % H_2 released from the sample of MgH_2@P/CMK-3 below 200 °C.

This work was supported by the National Natural Science Foundation of China (Nos. 51274139 and 51222402) and "Shu Guang" project supported by Shanghai Municipal Education Commission and Shanghai Education Development Foundation (13SG39). C.S. acknowledges the financial support from ARC Discover Project (DP130100268) and Future Fellowship (FT130100076). C.S. also appreciates the generous grants of CPU time from Australian National Computational Infrastructure.

[1]K.-F. Aguey-Zinsou and J.-R. Ares-Fernandez, Energy Environ. Sci. **3**(5), 526 (2010).
[2]L. Schlapbach and A. Züttel, Nature **414**, 353 (2001).
[3]X. D. Yao, C. Z. Wu, A. J. Du, J. Zou, Z. H. Zhu, P. Wang, H. M. Cheng, S. Smith, and G. Q. Lu, J. Am. Chem. Soc. **129**(50), 15650 (2007).

[4]N. Bazzanella, R. Checchetto, and A. Miotello, Appl. Phys. Lett. **92**, 051910 (2008).
[5]C. Z. Wu, P. Wang, X. Yao, C. Liu, D. M. Chen, G. Q. Lu, and H. M. Cheng, J. Alloys Compd. **414**(1–2), 259 (2006).
[6]C. Z. Wu, P. Wang, X. D. Yao, C. Liu, D. M. Chen, G. Q. Lu, and H. M. Cheng, J. Phys. Chem. B **109**(47), 22217 (2005).
[7]K. C. Kim, B. Dai, J. K. Johnson, and D. S. Sholl, Nanotechnology **20**, 204001 (2009).
[8]R. W. P. Wagemans, J. H. V. Lenthe, P. E. D. Jongh, A. J. V. Dillen, and K. P. D. Jong, J. Am. Chem. Soc. **127**, 16675 (2005).
[9]Z. G. Wu, M. D. Allendorf, and J. C. Grossman, J. Am. Chem. Soc. **131**(39), 13918 (2009).
[10]Z. Y. Li, G. S. Zhu, G. Q. Lu, S. L. Qiu, and X. D. Yao, J. Am. Chem. Soc. **132**(5), 1490 (2010).
[11]W. Y. Li, C. S. Li, H. Ma, and J. Chen, J. Am. Chem. Soc. **129**(21), 6710 (2007).
[12]K. Xia, Q. Gao, C. Wu, S. Song, and M. Ruan, Carbon **45**(10), 1989 (2007).
[13]L. Li, X. Yao, C. H. Sun, A. J. Du, L. N. Cheng, Z. H. Zhu, C. Z. Yu, J. Zou, S. C. Smith, P. Wang, H. M. Cheng, R. L. Frost, and G. Q. M. Lu, Adv. Funct. Mater. **19**(2), 265 (2009).
[14]T. K. Nielsen, U. Bosenberg, R. Gosalawit, M. Dornheim, Y. Cerenius, F. Besenbacher, and T. R. Jensen, ACS Nano **4**(7), 3903 (2010).
[15]S. F. Li, Y. H. Guo, W. W. Sun, D. L. Sun, and X. B. Yu, J. Phys. Chem. C **114**(49), 21885 (2010).
[16]H. Wang, S. F. Zhang, J. W. Liu, L. Z. Ouyang, and M. Zhu, Mater. Chem. Phys. **136**(1), 146 (2012).
[17]Y. Jia, C. Sun, L. Cheng, M. Abdul Wahab, J. Cui, J. Zou, M. Zhu, and X. Yao, Phys. Chem. Chem. Phys. **15**(16), 5814 (2013).
[18]D. S. Yang, D. Bhattacharjya, S. Inamdar, J. Park, and J. S. Yu, J. Am. Chem. Soc. **134**(39), 16127 (2012).
[19]R. Li, Z. D. Wei, X. L. Gou, and W. Xu, RSC Adv. **3**(25), 9978 (2013).
[20]J. P. Perdew, K. Burke, and M. Ernzerhof, Phys. Rev. Lett. **77**(18), 3865 (1996).
[21]G. Kresse and J. Joubert, Phys. Rev. B **59**(3), 1758 (1999).
[22]P. E. Blöchl, Phys. Rev. B **50**(24), 17953 (1994).
[23]S. Zhang, A. F. Gross, S. L. Van Atta, M. Lopez, P. Liu, C. C. Ahn, J. J. Vajo, and C. M. Jensen, Nanotechnology **20**, 204027 (2009).
[24]A. M. Puziy, O. I. Poddubnaya, R. P. Socha, J. Gurgul, and M. Wisniewski, Carbon **46**(15), 2113 (2008).
[25]Z. W. Liu, F. Peng, H.-J. Wang, H. Yu, W. X. Zheng, and J. Yang, Angew. Chem. Int. Ed. **50**(14), 3257 (2011).